Transient-State and Steady-State Kinetic Studies of the Mechanism of NADH-Dependent Aldehyde Reduction Catalyzed by Xylose Reductase from the Yeast *Candida tenuis*†

Bernd Nidetzky,* Mario Klimacek, and Peter Mayr

Division of Biochemical Engineering, Institute of Food Technology, Universität für Bodenkultur (BOKU), Muthgasse 18, A-1190 Vienna, Austria

Received January 23, 2001; Revised Manuscript Received May 29, 2001

ABSTRACT: Microbial xylose reductase, a representative aldo-keto reductase of primary sugar metabolism, catalyzes the NAD(P)H-dependent reduction of D-xylose with a turnover number approximately 100 times that of human aldose reductase for the same reaction. To determine the mechanistic basis for that physiologically relevant difference and pinpoint features that are unique to the microbial enzyme among other aldo/keto reductases, we carried out stopped-flow studies with wild-type xylose reductase from the yeast *Candida tenuis*. Analysis of transient kinetic data for binding of NAD^+ and NADH, and reduction of D-xylose and oxidation of xylitol at pH 7.0 and 25 °C provided estimates of rate constants for the following mechanism: E + NADH ⇄ E·NADH ⇄ *E·NADH + D-xylose ⇄ *E·NADH·D-xylose ⇄ *E·NAD^+·xylitol ⇄ *E·NAD^+ ⇄ E·NAD^+ ⇄ E + NAD^+. The net rate constant of dissociation of NAD^+ is ∼90% rate limiting for k_{cat} of D-xylose reduction. It is controlled by the conformational change which precedes nucleotide release and whose rate constant of 40 s^{-1} is 200 times that of completely rate-limiting *E·$NADP^+$ → E·$NADP^+$ step in aldehyde reduction catalyzed by human aldose reductase [Grimshaw, C. E., et al. (1995) *Biochemistry 34*, 14356−14365]. Hydride transfer from NADH occurs with a rate constant of approximately 170 s^{-1}. In reverse reaction, the *E·NADH → E·NADH step takes place with a rate constant of 15 s^{-1}, and the rate constant of ternary-complex interconversion (3.8 s^{-1}) largely determines xylitol turnover (0.9 s^{-1}). The bound-state equilibrium constant for *C. tenuis* xylose reductase is estimated to be ∼45 (=170/3.8), thus greatly favoring aldehyde reduction. Formation of productive complexes, *E·NAD^+ and *E·NADH, leads to a 7- and 9-fold decrease of dissociation constants of initial binary complexes, respectively, demonstrating that 12-fold differential binding of NADH (K_i = 16 μM) vs NAD^+ (K_i = 195 μM) chiefly reflects difference in stabilities of E·NADH and E·NAD^+. Primary deuterium isotope effects on k_{cat} and k_{cat}/K_{xylose} were, respectively, 1.55 ± 0.09 and 2.09 ± 0.31 in H_2O, and 1.26 ± 0.06 and 1.58 ± 0.17 in D_2O. No deuterium solvent isotope effect on k_{cat}/K_{xylose} was observed. When deuteration of coenzyme selectively slowed the hydride transfer step, $^{D_2O}(k_{cat}/K_{xylose})$ was inverse (0.89 ± 0.14). The isotope effect data suggest a chemical mechanism of carbonyl reduction by xylose reductase in which transfer of hydride ion is a partially rate-limiting step and precedes the proton-transfer step.

The catabolic pathway of D-xylose in yeasts and fungi starts with NAD(P)H-dependent reduction of D-xylose to xylitol, catalyzed by xylose reductase (XR).[1] Like well characterized mammalian aldose reductases, XR is a member of the aldo-keto reductase (AKR) superfamily (*1*, *2*). In the systematic classification of AKRs (*3*; for recent updates, see the AKR Webpage at the URL address http://www.med.upenn.edu/akr/) yeast XRs have been classified into subfamily 2B. The proposed catalytic mechanism of AKRs involves four active-site residues (Tyr/His/Lys/Asp) which cooperate to facilitate nucleophilic attack of the hydride ion to the *re*-side of the substrate carbonyl group [reviewed in ref *4* (*5*−*7*)]. The nicotinamide ring of NAD(P)H is positioned such that stereospecific transfer of the 4-pro-*R* hydrogen takes place. Positional conservation of tetrad residues Tyr-51, Lys-80, His-113, and Asp-46 in the enzyme from *Candida tenuis* (CtXR; AKR 2B5) and conserved A-side stereospecificity of hydride transfer (*8*) suggests a catalytic mechanism of xylose reductase common to other AKRs.

The turnover number of aldehyde reduction catalyzed by mammalian AR[1] is completely limited by a slow conformational change which precedes the release of $NADP^+$ (*9*, *10*). Crystallographic analysis of aldose reductase in complex with NADPH (*11*, *12*), AMP (*13*), and inhibitors (*14*−*17*) has provided strong support in favor of the suggestion that the kinetic "isomerization" step reflects structural rearrangements

† Supported by the Austrian Science Funds, Grant P-12569-MOB to B.N.

* To whom correspondence should be addressed. Phone: (+43)-1-36006-6274. Fax: (+43)-1-36006-6251. E-mail: nide@edv2.boku.ac.at.

[1] XR, xylose reductase; CtXR, xylose reductase from *Candida tenuis*; AR, aldose reductase; hAR, human aldose reductase; AKR, aldo-keto reductase; 3α-HSD, 3α-hydroxysteroid dehydrogenase; NADD, (4*R*)-[4²H]-NADD.

10.1021/bi010148a CCC: $20.00
Published on Web 07/27/2001

of the enzyme, including movement of loop B, made by residues Gly-213 to Leu-227, that folds over the nucleotide in the productive binary complex. Positional change of this loop from a closed (*E) to an open (E) position probably controls dissociation of the coenzyme (*9*−*11*). At equilibrium, the slow opening reaction contributes 100 and 650-fold to lowering the dissociation constants of the initial enzyme·nucleotide complexes (*9*). K_i values of NADPH and $NADP^+$ are thus in a low nanomolar range. Formation of a reactive *E·NADPH complex capable of reducing practically any, potentially toxic aldehyde, may be the physiological rational for the extremely tight binding of nucleotides by hAR (*18*).

The turnover number for reduction of D-xylose by CtXR ($k_{cat} \approx 17\ s^{-1}$)[2] is approximately 100 times that of human aldose reductase (hAR)[1] for the same reaction (*19*). By contrast, values of k_{cat}/K_{xylose} are similar for both enzymes indicating that high and low maximum rates have evolved with marginal changes in specificity. A recent comparative analysis of steady-state kinetic parameters of CtXR and hAR has underlined a specific physiological role of CtXR in the NAD(P)H-dependent reduction of D-xylose with high fluxional efficiency (*20*). Unlike hAR, CtXR was shown to utilize binding interactions with nonreacting parts of the aldehyde to bring about specificity for D-xylose *and* decrease the activation free energy for the rate-limiting step reflected by the value of k_{cat} (*20, 21*). k_{cat} in an ordered bi-bi mechanism such as that of CtXR (*19*) and hAR (*9*) is a function of all first order rate constants in the respective direction but only rate constants for the chemical step and product dissociation step depend on the substrate. In other words, since k_{cat} for CtXR shows significant variation across a series of structurally related aldehyde substrates (*20*), the net rate constants of steps involved in coenzyme release are probably not completely rate limiting for turnover by this enzyme.

The present paper reports experiments that were designed to advance the mechanistic basis for the observed differences in steady-state kinetic properties of CtXR and hAR, and characterize features of enzyme/substrate interaction that appear to be unique to XR among AKRs. Analysis of transient kinetic data recorded in stopped flow studies and simulation experiments were used to determine the complete kinetic mechanism of NADH-dependent reduction of D-xylose by the yeast enzyme and obtain estimates of microscopic rate constants. Isotope-effect studies were utilized to characterize the chemical step of carbonyl reduction pertaining to the relative timing of hydride transfer and proton transfer, and the relative contributions of hydride transfer and proton transfer to rate limitation for k_{cat} and k_{cat}/K_{xylose}.

A kinetic transient for binding of NADH and NAD^+ was observed for the first time with an aldo/keto reductase, which suggests that subtle differences exist in the mechanism of coenzyme binding used by individual members of the superfamily. The overall kinetic scheme of CtXR is found to be similar to that of hAR. Slow physical kinetic steps occur at the level of binary enzyme·nucleotide complexes, and they probably reflect conformational changes in enzyme structure. The most striking difference between CtXR and hAR pertains to the 200-fold faster rate constant of the conformational "isomerization" that precedes the release of $NAD(P)^+$. The physiological implications of that difference are discussed. A model of the chemical mechanism of carbonyl reduction by CtXR is presented which is based on isotope-effect data, and unique properties of XR are pointed out.

[2] Similar turnover numbers of 21 and 17 s^{-1} have been determined for CtXR-catalyzed reduction of D-xylose with NADPH and NADH as the coenzyme, respectively (*19*).

MATERIALS AND METHODS

Materials. If not mentioned otherwise, all materials were 99.5% pure. 2-Propanol-d_8 was from Sigma. A-side deuterium labeled NADH (NADD)[1] was prepared enzymatically (*22*). It was purified by anion exchange chromatography on a MonoQ column (Amersham Pharmacia). Analysis by ^1H NMR showed the deuterium content of NADD to be greater than 98%. D-*arabino*-2-Hexos-ulose ("D-glucosone"; 2-keto-D-glucose) was prepared from D-glucose using pyranose 2-oxidase from *Trametes multicolor* (*23*). Using analysis by TLC and HPLC, its purity was found to be 95%.

Enzymes. CtXR was purified to apparent homogeneity from cell extracts of *C. tenuis* CBS 4435 as described recently (*19*). Stock solutions of the enzyme in 50 mM Tris/HCl buffer, pH 7.0, containing 0.1% (w/v) Tween 20 were prepared by concentrating protein at 4 °C to about 10−20 mg/mL using a stirred Amicon ultrafiltration cell equipped with a YM 30 membrane. Protein was stored in aliquots at −70 °C. Before use, buffer was exchanged by gel filtration and if present, turbidity was removed by ultracentrifugation at 90000*g*. The molarity of solutions of CtXR was determined from measurements of the absorbance at 280 nm with a Hitachi U-3000 spectrophotometer and using a value of 54 000 $M^{-1}\ cm^{-1}$ for the molar extinction coefficient of CtXR at 25 °C, which is based on amino acid analysis (*8*).

Transient Kinetic Studies. Stopped-flow measurements were carried out with an Applied Photophysics instrument (model SX.18 MV) equipped with modular optical system. Data acquisition and analysis were done with Applied Photophysics software. When 100 μL was shot into a flow cell having a 1-cm path length, the fastest time for mixing two reactant solutions, introduced from two separate syringes, and recording the first data point was approximately 1.5 ms. All experiments were done in triplicate for each reactant concentration, and the resulting stopped-flow traces were averaged and then used for further analyses. Detection was by absorbance or fluorescence. Appropriate controls were recorded in all cases to exclude the possibility of artifacts. Reactions were carried out at 25 °C in 50 mM potassium phosphate buffer, pH 7.0, using final concentrations of the enzyme (based on a molecular mass of 36 kDa) that were constant across a series of reactant concentrations but otherwise varied between 5.5 and 16.9 μM. Binding of NAD^+ and NADH was measured as quenching of intrinsic protein fluorescence which occurred upon mixing of enzyme solution and nucleotide solution from two separate syringes. The excitation wavelength was at 295 nm and the emission wavelength was at 335 nm The nucleotide concentrations employed ranged between 25 and 1000 μM NAD^+ and 5−100 μM NADH and binding was monitored for 5−6 different concentrations of NAD(H). The absorbance of NADH at 335 nm leads to significant quenching of tryptophan fluorescence in the absence of true binding, and

therefore, NADH concentrations greater than 100 μM were not used. For measurement of multiple turnover transients, enzyme (11−22 μM) was premixed with saturating concentrations of NADH (110 μM) or NAD^+ (1.5 mM) in one syringe, and the other syringe contained the substrate solution (0.08−1.5 M D-xylose or xylitol) plus nucleotide at the same concentration as in the enzyme solution. Therefore, the final concentration of nucleotide (110 μM NADH, 1.5 mM NAD^+) did not change upon mixing the two solutions. For measurement of single turnover transients, the enzyme reservoir contained 14.2 μM CtXR and optionally, the same or a smaller concentration of nucleotide. The final concentration of substrate in single and multiple turnover transients was adjusted by varying [D-xylose] (not the volume) added from the syringe containing the substrate solution. Reactions were monitored from the change in absorbance at 340 nm (ϵ = 6220 M^{-1} cm^{-1}).

Nucleotide Binding to CtXR Monitored by Fluorescence. Steady-state fluorescence measurements were carried out at 25 ± 1 °C equipped with a Hitachi F-2000 spectrofluorometer with a thermostated cell compartment. Fifty millimolar Tris or 50 mM potassium phosphate buffer, both pH 7.0, were used as indicated. Binding of NAD^+ was determined by measuring the quenching of intrinsic tryptophan fluorescence of CtXR, as described above. The enhancement of nucleotide fluorescence (em, 450 nm; ex, 340 nm) on binding to CtXR was used to determine the dissociation constant of the enzyme·NADH complex. The fluorescence titrations were carried out at an enzyme concentration of 8.3 μM. Measurements were done after adding a 2−5 μL aliquot from concentrated stock solutions (1 mM NADH, 3 mM NAD^+), and appropriate corrections for dilution were made. Controls were obtained by the same procedure without enzyme, and corrections for the blank values at the corresponding nucleotide concentrations were made in all cases. Scatchard analysis was used to determine the dissociation constant of the binary enzyme·nucleotide complexes as well as the number of NADH binding sites in CtXR on a molar basis.

Steady-State Kinetic Studies. Experiments were performed at 25 °C in 50 mM potassium phosphate buffer, pH 7.0. Initial rates were measured with a Beckman DU-640 spectrophotometer recording the depletion of NADH at 340 nm. Control assays containing the enzyme and NADH, and NADH and the substrate ensured that blank rates were negligible under the conditions employed. The total volume per assay was 1 mL, and reactions were initiated by adding 20 μL of NADH, dissolved in water. All initial velocity data were obtained under conditions in which one substrate was varied at a constant and saturating concentration of the second substrate. Primary deuterium kinetic isotope effects on apparent kinetic parameters for aldehyde reduction were obtained by using NADD. Deuterium solvent isotope effects were determined at saturating concentrations of NADH or NADD using D-xylose or D-glucosone as the varied substrate. Phosphate buffer with D_2O were brought to "pH" with DCl using correction for the isotope effect on the response of the pH electrode according to pD = meter reading + 0.4 (*24*).

Data Processing. Reciprocal initial velocities were plotted vs reciprocal substrate concentrations, and the experimental data were fitted to eqs 1−8 by the least-squares method, and using the Sigmaplot program, ver. 5, for Windows (Jandel). The correlation coefficient of regression analysis was generally greater than 0.985, and unless mentioned otherwise problems with strongly correlated parameter estimates were not observed. Linear double reciprocal plots were fitted to eq 1 where v is the initial rate, E is the enzyme and A is the substrate, k_{cat} is the turnover number and K_A is the apparent Michaelis constant for A.

$$v = k_{cat}[E][A]/(K_A+[A]) \quad (1)$$

Equation 2 was used to determine isotope effects when one substrate was varied, where $E_{V/K}$ and E_V are the isotope effects minus 1 on k_{cat}/K_A and k_{cat}, respectively. The fraction of deuterium in the labeled substrate or the solvent is given by F_i.

$$v = k_{cat}[E][A]/[K_A(1 + F_iE_{V/K}) + [A](1 + F_iE_V)] \quad (2)$$

Pseudo-first-order rate constants of kinetic transients (k_{obs}) were calculated from single- or double-exponential fits to averaged stopped-flow traces using Applied Photophysics software, based on nonlinear regression algorithm. The decision of whether a double exponential fit the data significantly better than a single exponential was based on variance analysis, the confidence intervals of the estimates for k_{obs} and the statistical correlation of parameter estimates. When general saturation behavior was observed, eq 3 was used to fit the data whereby k_{max} is the maximum rate constant and K_A^{app} is an apparent half-saturation constant.

$$k_{obs} = k_{max}[A]/(K_A^{app} + [A]) \quad (3)$$

Results for a two-step binding mechanism of nucleotides (eq 4) in which the first step is fast relative to second step, were analyzed by using eqs 5 and 6.

$$E + Nu \rightleftarrows E{\cdot}Nu \rightleftarrows {}^*E{\cdot}Nu \quad (4)$$

$$k_{obs,1} = k_2 + k_1[Nu]_{tot} \quad (5)$$

$$k_{obs,2} = k_4 + k_3[Nu]_{tot}/(K_d + [Nu]_{tot}) \quad (6)$$

where $k_{obs,1}$ and $k_{obs,2}$ are observed rate constants for the fast and slow kinetic transient, Nu and Nu_{tot} are free and total nucleotide concentrations, respectively, and K_d ($=k_2/k_1$) is a dissociation constant. Rate constant numbering refers to eq 4 whereby k_1 and k_2 and k_3 and k_4 relate to the first and second step of binding, respectively. Since binding of NADH is tight relative to the enzyme concentration used in our experiments (5.5−16.9 μM), eq 7 was used to analyze the data.

$$k_{obs} = k_4 + k_3E_{NADH}/E_{tot} \quad (7)$$

where E_{NADH}/E_{tot} is the fraction of enzyme liganded with NADH, and E_{NADH} is given by eq 8.

$$E_{NADH} = \{(K_d + [E]_{tot} + [Nu]_{tot}) - [(K_d + [E]_{tot} + [Nu]_{tot})^2 - 4[E]_{tot}[Nu]_{tot}]^{1/2}\}/2 \quad (8)$$

Rate constants for coenzyme binding were obtained by using nonlinear fits of eqs 5−8 to experimental data. Alternative graphical procedures were not used.

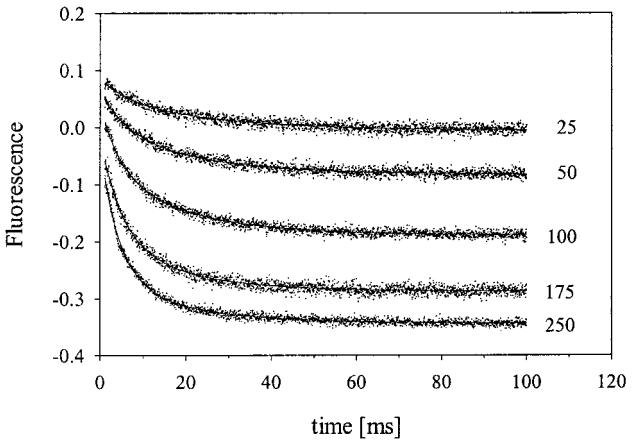

FIGURE 1: Representative kinetic transients of NAD^+ binding to CtXR measured as quenching of protein fluorescence in a stopped-flow experiment. Reactions were carried out at 25 °C in 50 mM potassium phosphate buffer, pH 7.0, using 7.0 μM enzyme and NAD^+ at the concentrations in μM indicated. Solid lines are double exponential fits of the data.

Simulation of Transient-State Reactions. Experimental stopped-flow progress curves of nucleotide binding and enzymatic reactions with D-xylose and xylitol were analyzed by using the interactive simulation program KINSIM (*25*). KINSIM simulations used the observed values of rate constants and the actual starting concentrations of enzyme, coenzyme, and substrate. Comparison of experimental and simulated progress curves was used to obtain estimates for rate constants which were not directly observable in stopped-flow measurements.

RESULTS

Kinetic Transients of Nucleotide Binding. To characterize binding of NAD^+ and NADH to CtXR, we carried out transient-state kinetic studies by using fluorescence stopped-flow measurements. Fluorescence traces were recorded at varied [NAD^+] or [NADH], and quenching of intrinsic tryptophan fluorescence at 335 nm (following excitation at 295 nm) served as reporter of the binding event. Representative progress curves of binding of NAD^+ are shown in Figure 1. The curves were in all cases fit best by two exponentials, reflecting a fast phase and a second slower phase of binding. Biphasic transient-rate behavior is fully consistent with a two-step mechanism of nucleotide binding in which rapid formation of a weak complex, E·NAD^+, precedes the slow formation of the more stable, productive *E·NAD complex (see eq 4). Rate constants (k_{obs}) for the fast and slow transient were calculated at each [NAD^+], and the analysis of k_{obs} in dependence on nucleotide concentration is shown in Figure 2. As expected for a two-step mechanism (cf. eqs 4 and 5), a plot of k_{obs} of the fast phase against the NAD^+ concentration was linear. A straight line fit to the data had a slope of $(0.17 \pm 0.02) \times 10^6$ M^{-1} s^{-1} (corresponding to k_1) and a y-axis intercept of 263 ± 73 s^{-1} (corresponding to k_2). Therefore, K_d ($=k_2/k_1$) is 1.55 mM. The wide range of nucleotide concentrations used in the experiments rules out that saturation with NAD^+ would have escaped detection. The plot of k_{obs} of the second phase shows saturation at high concentrations of NAD^+, as required by the mechanism (eq 4). Equation 6 with a fixed value of 1.55 mM for K_d was used to fit by nonlinear regression the data for the range 50−500 μM NAD^+ and determine k_3 (273 ± 111 s^{-1}) and k_4 (40 ± 9 s^{-1}). The data obtained at very high NAD^+ were not used in the calculation because the value of k_{obs} slightly decreased when NAD^+ was present at 500 μM or greater. This decrease may be caused by the increasing filter effect at high [NAD^+]. It is most probably not due to specific binding interactions of CtXR and NAD^+ and was not further pursued.

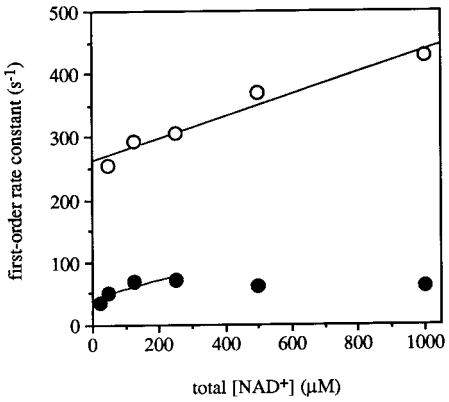

FIGURE 2: Dependence on NAD^+ concentration of first-order rate constants (k_{obs}) for fast (open circles) and slow (full circles) kinetic transient of nucleotide binding. Values of k_{obs} showed standard deviations of less than 10%.

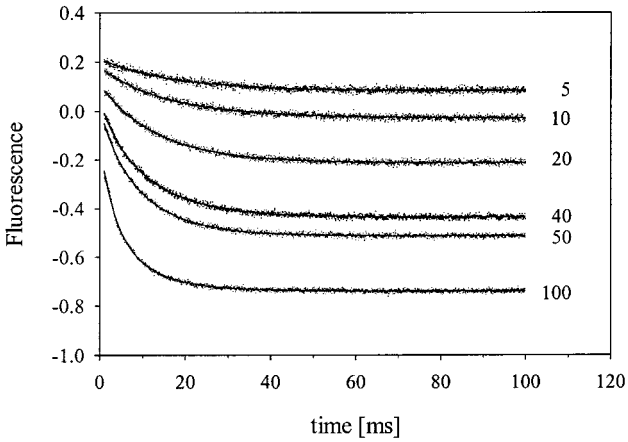

FIGURE 3: Representativekinetic transients of NADH binding to CtXR measured as quenching of protein fluorescence in a stopped-flow experiment. Reactions were carried out at 25 °C in 50 mM potassium phosphate buffer, pH 7.0, using 16 μM enzyme and NADH at the concentrations in μM indicated. Solid lines are double exponential fits of the data.

Fluorescence stopped-flow traces observed upon mixing CtXR and NADH are shown in Figure 3. Experimental progress curves were best described by two exponentials,[3] indicative of a two-step binding mechanism of NADH closely similar to that of NAD^+. However, since quenching of tryptophanyl fluorescence can be caused by enzyme-bound *and* free NADH, the narrow range of useful nucleotide concentrations limited the analysis of k_{obs} in dependence of [NADH]. k_{obs} for the fast phase showed a linear dependence on [NADH]. A straight line fit to the data yielded a slope of $(1.70 \pm 0.20) \times 10^6$ M^{-1} s^{-1} (corresponding to k_1) and an

[3] At [NADH] of between 5 and 15 μM, it was difficult to distinguish whether a double exponential fit the kinetic transient better than a single exponential.

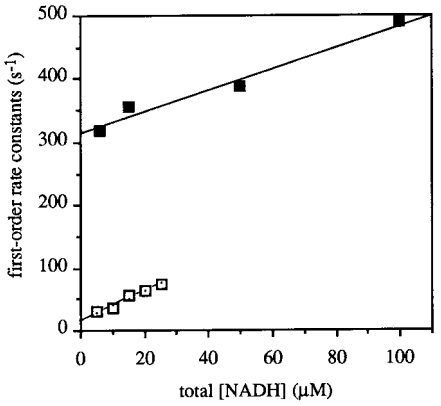

FIGURE 4: Dependence on NADH concentration of first-order rate constants (k_{obs}) for fast (full squares) and slow (open squares) kinetic transient of nucleotide binding. Values of k_{obs} showed standard deviations of less than 10%.

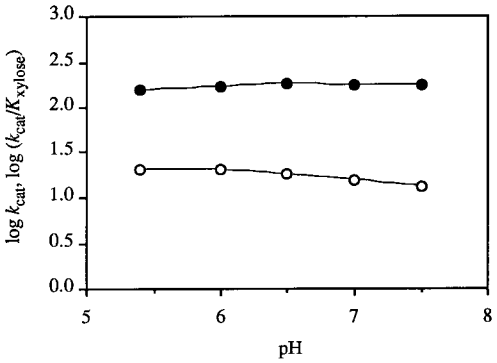

FIGURE 5: pH profiles for the NADH-dependent reduction of D-xylose catalyzed by CtXR. Reactions were carried out at 25 °C in 50 mM potassium phosphate buffer using 220 μM NADH. Kinetic parameters (k_{cat}, open circles; k_{cat}/K_{xylose}, full circles) were obtained from nonlinear fits of initial velocities to eq 1. Lines indicate the trend of the data.

intercept of 315 ± 30 s^{-1} (corresponding to k_2). k_{obs} for the slower phase was dependent on [NADH] (Figure 4), and eq 8 was employed to fit the data for [NADH] ≤ 25 μM using a fixed value of 185 μM for K_d ($=k_2/k_1$). The strong statistical correlation between the amplitude and k_{obs} for the slower phase limited the useful range of [NADH]. Estimates of 135 ± 15 and 15 ± 4 s^{-1} were obtained for k_3 and k_4, respectively. If one compares the rate constant ratio k_3/k_4 for binding of NAD^+ and NADH, a similar 7- and 9-fold tightening is observed on formation of the productive *E• nucleotide complex, respectively.

Steady-State Nucleotide Binding. Scatchard analysis of the data obtained for binding of NADH and NAD^+ gave K_i values of 12 ± 2 and 290 ± 45 μM, respectively. The binding studies showed that CtXR has a single binding site for NADH per each 36-kDa enzyme protomer (1.10 ± 0.15). The stability of the enzyme•NAD^+ complex was too weak to obtain a reliable value of stoichiometry of binding of NAD^+.

Isotope-Effect Studies at the Steady State. Initial velocities of aldehyde reduction were measured in H_2O in the presence of a saturating concentration of NADH or NADD to determine the primary deuterium kinetic isotope effects on k_{cat} and $k_{cat}/K_{aldehyde}$. They were recorded in D_2O to determine the solvent isotope effects on the same kinetic parameters. Since experiments were carried out in pH(D) range where both k_{cat} and k_{cat}/K_{xylose} do not show significant pH dependence (Figure 5), observable solvent isotope effect are real and do not reflect differences in pL profiles of kinetic parameters recorded in H_2O and D_2O. Multiple deuterium kinetic isotope effects were also obtained in these experiments. Equation 2 was fitted to the data, and results are summarized in Table 1. When NADH and NADD were varied and D-xylose was constant and saturating (700 mM), there was no significant isotope effect on k_{cat}/K_{NADH} (1.00 ± 0.06). This finding is in excellent agreement with requirements of an ordered bi−bi mechanism of CtXR (*19*) where the rate of release of NADH from the ternary enzyme/substrate complex is expected to have a near zero value. At saturating concentrations of D-xylose, the forward commitment to catalysis (*27*) will thus be infinite and so the isotope effect on k_{cat}/K_{NADH} is completely masked. A value of 1.49 ± 0.06 has been determined for $^Dk_{cat}$ in the experiment with varied nucleotide. It is in good agreement with data reported in Table 1. $^{D_2O}k_{cat}$ and $^{D_2O}(k_{cat}/K_{xylose})$ were not significantly different from a value of 1 whereas the solvent isotope effect on k_{cat} measured with D-glucosone was 1.30. Note that $^{D_2O}(k_{cat}/K_{glucosone})$ was 1.

Multiple Turnover Reactions. Figure 6 shows a representative set of progress curves measured using NADH or NADD at a concentration of 110 μM which is saturating (~7 × K_{NADH}) and allows multiple turnovers of the enzyme. The reactions were followed by measuring the decrease in A_{340nm} due to the oxidation of NADH. Results are displayed for a D-xylose concentration of 150 mM which equals 2 × K_{xylose} and one of 750 mM which is saturating in the steady state. Note that the enzyme was presaturated with nucleotide in these experiments. For D-xylose concentrations of between 40 and 750 mM, the disappearance of NADH with time was characterized by a short initial lag that preceded the actual (exponential) kinetic transient which in turn was followed by a linear steady-state phase of reaction (Figure 6). The lag time decreased with increasing [D-xylose] suggesting that under these conditions, the rate of substrate binding is rate limiting for the transient rate. Typically, the steady-state rate was attained after approximately 40 ms. The zero-order rate constant (k_{ss}) was calculated from $\Delta A_{340nm}/\Delta t$ in the linear phase of reaction. Its dependence on substrate concentration showed saturation at high [D-xylose]. A nonlinear fit of eq 1 to experimental data yielded values of 15 ± 2 s^{-1} for k_{cat} and 76 ± 8 mM for K_{xylose}, in very good agreement with results obtained from analysis of initial-velocity data. The isotope effect on k_{ss} measured at a saturating D-xylose concentration of 750 mM was 1.80, corresponding reasonably with a value of 1.56 for $^Dk_{cat}$ in Table 2.

In reverse reaction catalyzed by CtXR, multiple turnover progress curves for xylitol oxidation did not show a pre-steady-state burst or lag. They were characterized by the linear appearance of NADH absorbance, and values for k_{ss} were calculated from these data. The dependence of k_{ss} on xylitol concentration was hyperbolic, and a fit of eq 3 to data of k_{ss} vs [xylitol] gave k_{cat} = 0.92 ± 0.23 s^{-1} and $K_{xylitol}$ = 192 ± 59 mM, in agreement with results of conventional initial-velocity studies.

Single-Turnover Reactions. Stopped-flow measurements were carried out under conditions where the concentration of NADH or NADD constrained the reaction to a single turnover of the enzyme present (14.2 μM). Absorbance traces

Table 1: Primary Deuterium and Deuterium Solvent Isotope Effects on Kinetic Parameters of Aldehyde Reduction Catalyzed by CtXR[a]

	$^{D}k_{cat}$[b]	$^{D}(k_{cat}/K)$	$^{D_2O}k_{cat}$[b]	$^{D_2O}(k_{cat}/K)$
D-xylose	H_2O:[c] 1.55 ± 0.09	H_2O: 2.09 ± 0.31	NADH:[d] 1.04 ± 0.06	NADH: 0.97 ± 0.12
	D_2O:[c] 1.26 ± 0.06	D_2O: 1.58 ± 0.17	NADD:[d] 0.82 ± 0.05	NADD: 0.89 ± 0.14
D-glucosone	H_2O: 1.22 ± 0.06	H_2O: 1.64 ± 0.21	NADH: 1.30 ± 0.04	NADH: 1.11 ± 0.09[e]

[a] The nomenclature of Northrop (*26*) is used, whereby $^{D}k_{cat}$ and $^{D}(k_{cat}/K)$ are primary deuterium isotope effects on k_{cat} and k_{cat}/K, and $^{D_2O}k_{cat}$ and $^{D_2O}(k_{cat}/K)$ are the corresponding solvent isotope effects. [b] [NADH] and [NADD] were saturating at 220 μM ($\sim 15 \times K_{NADH}$). [c] Primary deuterium isotope effect measured in H_2O or D_2O. [d] Solvent isotope effect measured with NADH or NADD. [e] *t*- and *P*-test statistics show that this value is not significantly different from 1.

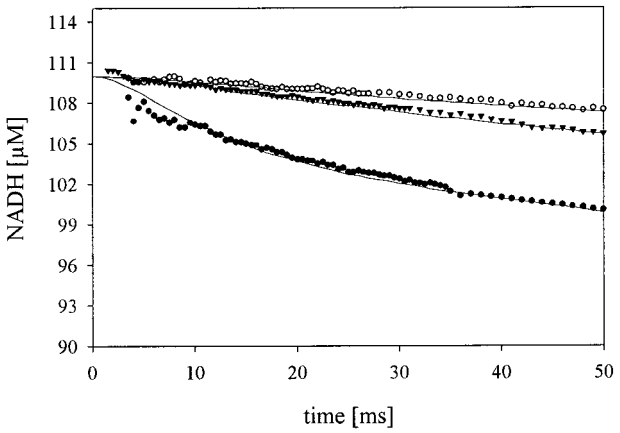

FIGURE 6: Representative progress curves of NADH-dependent reduction of D-xylose in multiple-turnover stopped flow experiments. Reactions were carried out at 25 °C in 50 mM potassium phosphate buffer, pH 7.0, using 11 μM enzyme and 110 μM NADH. Results are shown for [D-xylose] of 750 mM (full circles) and 150 mM (full triangles) using NADH. Open circles show the reaction at 750 mM D-xylose using 5.5 μM enzyme and 110 μM NADD. Solid lines were calculated for the mechanism in Scheme 1 using KINSIM and the rate constants in Table 3, considering that the enzyme was preincubated with NADH or NADD before starting the reaction.

were recorded in the presence of [D-xylose] of between 40 and 300 mM, and the decrease in A_{340nm} was in all cases best fit by a single exponential.[4] The amplitude (ΔA_{340nm}) was independent of the [D-xylose] and corresponded to the total concentration of NADH or NADD oxidized (7.0 μM). The first-order rate constants (k_{trans}) calculated from the kinetic transients showed a linear dependence on [D-xylose] (not shown), yielding slope values of 46 and 19 M^{-1} s^{-1} for experiments conducted with NADH and NADD, respectively. These slopes correspond to k_{max}/K^{app}_{xylose} for the transient reactions. Thus $^{D}(k_{max}/K^{app}_{xylose}) = 2.42$, which indicates that hydride transfer makes a substantial contribution to rate limitation of the single turnover transient rate.

KINSIM Analysis of Progress Curves. Progress curves obtained in multiple and single-turnover stopped-flow measurements were analyzed using KINSIM and assuming the mechanism shown in Scheme 1 (as discussed later). Values of k_1-k_4 and $k_{11}-k_{14}$ were those from transient-state binding studies with NADH and NAD^+ (see Table 2). The "on" and "off" rate constants of xylitol do not appear to contribute to rate limitation in reverse and forward reaction catalyzed by CtXR, respectively (see the Discussion). Therefore, k_9 and k_{10} were set at values high enough to be kinetically transparent with the constraint that k_9/k_{10} equals $K_{xylitol} \approx$ 200 mM (*19*). An estimate of 170 s^{-1} for the hydride transfer rate constant (k_7) was calculated as follows. Release of NAD^+ takes place with a net rate constant ($k'_{11,13}$) of 18.6 s^{-1}. Now, assuming that the value of 6.5 for the intrinsic isotope effect of NADPH-dependent D-xylose reduction catalyzed by hAR [$^{D}k_7$ (*9*)] is applicable to the corresponding NADH-dependent reaction of CtXR, the relationship $^{D}k_{cat} = 1.55 = {}^{D}k_7 + C_{Vf}/(1 + C_{Vf})$ was used to obtain an estimate of 9 for C_{Vf} (which is a rate constant ratio and will be discussed later). In its simplest form, $C_{Vf} \approx k_7/k'_{11,13}$ and thus $k_7 \approx 170$ s^{-1}. Dependence of k_{trans} on [D-xylose] and isotope effects on k_{cat}/K_{xylose} were used to obtain estimates for k_5 ($\sim$200 M^{-1} s^{-1}) and k_6 ($\sim$55 s^{-1}), respectively. The net rate constant of xylitol oxidation, $k'_8 = k_8k_6/(k_6 + k_7)$, was constrained to a value of of 0.92 s^{-1} which equals k_{cat} in this direction, and thus $k_8 \approx$ 3.76 s^{-1}. Values for microscopic rate constants are summarized in Table 2. Simulated progress curves using the above rate constants for k_1-k_{14} are shown in Figure 6 where they are compared to experimental data obtained with NADH in multiple-turnover reactions. In the reactions with NADD, only k_7 and k_8 were allowed to vary because k_5 and k_6 were assumed to be independent of deuteration of nucleotide. k_{8D} was calculated from $^{D}k_7$ by using the relationship, $k_{8D} = k_{8H}{}^{D}K_{eq}/{}^{D}k_7$ whereby $^{D}K_{eq} = 0.93$ is the equilibrium isotope effect for NAD(P)D-dependent reduction of an aldehyde (*28*).

Table 2: Estimates of Microscopic Rate Constants for NADH-Dependent Reduction of D-Xylose and NAD^+-Dependent Oxidation of Xylitol Catalyzed by CtXR

k_1	$(1.7 \pm 0.2) \times 10^6$ M^{-1} s^{-1}	k_2	315 ± 34 s^{-1}
k_3	134 ± 15 s^{-1}	k_4	15 ± 4 s^{-1}
k_5	200 M^{-1} s^{-1} (1.0×10^6 M^{-1} s^{-1})[a,b]	k_6	55 s^{-1} [b,c]
k_7	170 s^{-1} (26 s^{-1})[b,c]	k_8	3.8 s^{-1} (0.54 s^{-1})[b]
k_9	1×10^5 s^{-1}	k_{10}	5×10^5 M^{-1} s^{-1}
k_{11}	40 ± 9 s^{-1}	k_{12}	273 ± 111 s^{-1}
k_{13}	263 ± 73 s^{-1}	k_{14}	$(0.17 \pm 0.02) \times 10^6$ M^{-1} s^{-1}

[a] Value obtained when correction is made for the 0.02% free aldehyde form in aqueous solution of D-xylose (*45*). [b] Sensitivity analysis for k_5-k_8 was carried out in which the values for the rate constants were changed systematically within a 0.5−1.5-fold range of the reported value; k_5 and k_6 make the major contribution to the dependence of k_{obs} on [D-xylose] and the observed progress curves in multiple and single turnover reactions; the estimated values for k_5 and k_6 are ±20%. [c] Values in parentheses are k_{7D} and k_{8D} assuming a value of 6.5 (*9*) for the intrinsic isotope effect ($^{D}k_7$), in good agreement with results of KINSIM analysis of progress curves for reduction of D-xylose with NADD (see Figure 6).

[4] When [D-xylose] was between 300 and 750 mM, the observed initial $A_{340\ nm}$ was up to 3 times larger than the value expected from total [NADH] present. A decrease of A_{340nm} to a value corresponding to [NADH] occurred within a 3-ms long incubation time. k_{obs} for this decrease was approximately 1500 s^{-1}. Reactions containing or lacking the enzyme yielded identical absorbance traces in this initial phase, suggesting that with the instrument used, mixing two solutions of which one contains 0.6 or 1.5 M D-xylose requires about 3 ms to proceed to completion (not shown). At [D-xylose] = 300 mM, analysis of progress curves was therefore done for $t > 3$ ms.

Scheme 1

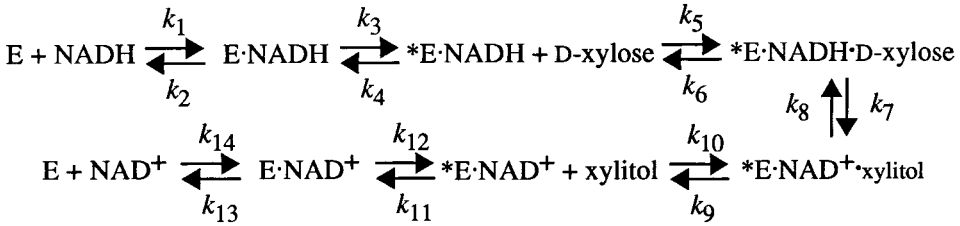

Results of the simulation for reaction with NADD are shown in Figure 6.

DISCUSSION

Overall Kinetic Scheme of Xylose Reductase. Analysis of transient kinetic data for binding of NADH and NAD^+, and reduction of D-xylose and oxidation of xylitol reveals an expanded ordered kinetic mechanism for this enzyme, as shown in Scheme 1. Estimates of microscopic rate constants were obtained that allow one to accurately model stopped-flow progress curves and calculate values of steady-state constants that agree well with those obtained in conventional binding and initial-velocity studies. The reaction mechanism of CtXR is characterized by the occurrence of two slow, physical kinetic steps which probably reflect conformational changes of CtXR at the level of binary enzyme·nucleotide complexes. At saturating concentrations of D-xylose and NADH, the rate of dissociation of *E·NAD^+ to give E + NAD^+ accounts for ~90% of rate limitation for the forward turnover number in the steady state. Hydride transfer from NADH is only ~10% rate limiting for k_{cat}. In the transient state, however, the net rate constant for substrate binding, k'_5 ($=k_5k'_7$[D-xylose]/($k_6 + k'_7$) whereby $k'_7 \approx k_7$) chiefly controls the observed rate over a wide range of substrate concentrations. This result explains the absence of a detectable pre-steady-state burst of NADH consumption in multiple-turnover stopped-flow measurements conducted with CtXR at [D-xylose] ≤ 750 mM. In reverse reaction, chemistry of ternary-complex interconversion by hydride transfer from xylitol is the slowest step and its net rate constant equals k_{cat} of ~1 s^{-1} in this direction.

Release of Xylitol Is Not Rate Limiting for Transient Rate of D-Xylose Reduction. Contrary to binding of NAD^+ and NADH, binding to CtXR of aldehyde or alcohol was fluorescently silent (results not shown), and therefore, the observed rate constants for the transient kinetic phases in single and multiple turnover experiments required interpretation so as to derive the mechanism in Scheme 1. In single-turnover experiments of D-xylose reduction, each of the steps from substrate binding to release of the alcohol product contributes to transient rate behavior. In a theoretical analysis of the ordered kinetic mechanism of NAD^+-dependent dehydrogenases (*29*), it has been shown that at saturation with the second substrate, the relative magnitudes of rate constants k_7-k_9 determine whether the pre-steady-state rate will be biphasic or occur in a single phase. When k_7 is much smaller than $k_8 + k_9$, a single transient with an amplitude corresponding to the concentration of the limiting reactant is expected. On the other hand, when $k_7 \approx k_8 + k_9$, a fast and slow transient will be observed. In such a case, the amplitudes of both transients will be of significant magnitude and dependent on the substrate concentration used, as shown for reduction of benzaldehyde by liver alcohol dehydrogenase (*30, 31*). Transient kinetics of NADH-dependent D-xylose reduction by CtXR are best described by a single exponential with an amplitude corresponding to the concentration of the limiting [NADH]. Now, because the rate constant of xylitol oxidation, k_8, must be much smaller than k_7 or k_9, it follows that $k_9 \gg k_7$, suggesting a mechanism of CtXR in which the rate of xylitol dissociation is much faster than the rate of xylitol formation by ternary-complex interconversion.

Isotope Effects. When NADD is used in place of NADH for reduction of D-xylose, a significant primary deuterium isotope effect is observed on k_{cat} and k_{cat}/K_{xylose}, and on the kinetic transient rate constant, k_{max}/K^{app}_{xylose}. Qualitatively, this indicates that hydride transfer contributes to rate limitation of the catalytic sequence of CtXR and is also a slow step of the overall steady-state reaction as well as the transient reaction. The observation of an isotope effect on k_{cat} that is smaller than the isotope effect on k_{cat}/K_{xylose} suggests a mechanism in which the rates of chemical reduction and nucleotide release are partially rate limiting for k_{cat}. In the detailed analysis of isotope effects, however, it is most useful to consider how individual rate constants in the form of commitment factors contribute to reduce the intrinsic isotope effect on the catalytic step of hydride transfer ($^Dk_7$) to the experimentally observed isotope effect on rate constants or kinetic parameters (for reviews, see refs *27* and *32*).

We shall discuss first the isotope effect on k_{cat}. Since there is only one isotope-sensitive step in the mechanism, we can write

$$^Dk_{cat} = (^Dk_7 + C_{Vf} + C_r\,^DK_{eq})/(1 + C_{Vf} + C_r)$$

where C_{Vf} is a comparison between the rate constant for the isotope-sensitive step and rate constants for all other forward unimolecular steps, and C_r is the reverse commitment factor, respectively. C_r is given by the ratio k_8/k_9. It is very small and does not contribute to the value of $^Dk_{cat}$. The expression for C_{Vf} is

$$C_{Vf} = k_7[(1/k_3) + (1/k_9) + (1/k_{11})(1 + k_{12}/k_{13}) + (1/k_{13})]$$

and by using the rate constants from Table 3 we calculate $C_{Vf} = 10.6$ and therefore $^Dk_{cat} = 1.47$, corresponding to a value of 1.55 for $^Dk_{cat}$ determined from initial-velocity measurements.

The isotope effect on k_{cat}/K_{xylose} and k_{max}/K^{app}_{xylose} is given by the relationship

$$^D(k_{cat}/K_{xylose}) = (^Dk_7 + C_f + C_r\,^DK_{eq})/(1 + C_f + C_r)$$

where C_f is the forward commitment factor and equals the expression k_7/k_6. The calculated value of $C_f = 3.1$ and

Table 3: Comparison of Calculated and Measured Kinetic Parameters for CtXR

parameter	calculated[a]	measured[b]
k_{cat} (D-xylose) (s^{-1})	14.8	14.2[c]
K_{NADH} (μM)	29	15
K_{xylose} (mM)	108	78
$K_{i,NADH}$ (μM)	19	16 (12)[d]
k_{cat} (xylitol) (s^{-1})	0.84	0.92[c]
$K_{NAD}+$ (μM)	10 (23)[e]	27
$K_{xylitol}$ (mM)	206	209
$K_{i,NAD}+$ (μM)	198 (554)[e]	195 (290)[d]

[a] Using relationships of microscopic rate constants to kinetic parameters derived by using the concept of net rate constants (*9*, *46*). [b] Data from ref *19* assuming a molecular mass of 36 kDa for CtXR. [c] This work. [d] Data from fluorescence titration. [e] Data calculated by using the maximum *observable* value of 72 s^{-1} for k_3.

therefore, $^{D}(k_{cat}/K_{xylose}) = {}^{D}(k_{max}/K^{app}_{xylose}) = 2.34$, in good agreement with the experimental values. The data predict that D-xylose is a sticky substrate of CtXR; i.e., it reacts to give product at a rate faster than the net rate of dissociation from the ternary complex (for the general case, see ref *27*).

Comparison of Nucleotide-Induced Conformational Changes in CtXR and Other Aldo/Keto Reductases. Transient kinetics of nucleotide binding have been studied with mammalian aldose reductase (*9*, *10*), 3α-hydroxysteroid dehydrogenase (*33*; 3α-HSD; AKR 1C9), and CtXR (this work). In all cases, results provide strong support in favor of a two-step binding mechanism where a conformational change in enzyme structure is required for formation of the productive binary complex and causes a decrease in K_d for the initial complex of enzyme and nucleotide. The X-ray structure of hAR (*11*) is in good agreement with the interpretation of the kinetic events, suggesting that movement and ordering of a mobile loop are triggered through anchoring the coenzyme in the active site. The second, slow kinetic transient revealed in stopped-flow progress curves of coenzyme binding by porcine AR (*10*) likely has causal relationship to the positional change of this loop. However, as shown for 3α-HSD (*33*), it may not be a direct reporter of this event. In case of 3α-HSD which utilizes NADPH and NADH, the kinetic transient was NADPH-specific and could be abolished through mutation of Arg-276, which provides an electrostatic linkage with the 2′-phosphate group of AMP, thus serving as the "anchor" for NADP(H) binding (*33*, *34*). Arg-276 of 3α-HSD is positionally conserved in CtXR (*8*). The results for CtXR present the first report of a kinetic transient upon binding of NADH and NAD^+ to an AKR member. It seems, therefore, that (subtle) differences prevail among individual aldo/keto reductases with regard to the molecular mechanisms underlying the observable kinetic events during coenzyme binding.

The magnitude of the "conformational tightening" in the binding of NAD(P)H (k_3/k_4) and $NAD(P)^+$ (k_{12}/k_{11}) is determined mainly by the rate constant for the rearrangement from the closed to the open position and distinguishes among individual AKR members. It is in a 10-fold range for 3α-HSD (*33*) and CtXR, but in a 100−1000-fold range for hAR (*9*). The opening rate constant for $*E{\cdot}NAD(P)^+$ (k_{11}) is very small for hAR (0.2 s^{-1}) but considerably greater for CtXR (40 s^{-1}) and 3α-HSD (11 s^{-1}). Note that unlike hAR, the net rate constant of release of $NAD(P)^+$ is not completely rate limiting for k_{cat} of NAD(P)H-dependent carbonyl reduction catalyzed by CtXR and 3α-HSD. Sequence comparison of CtXR and hAR, based on hAR X-ray structures (*11*), provides a plausible explanation of the 200-fold (40/0.2) difference in the rate constant k_{11}, as follows. In hAR, salt-link interactions of Asp-216 with Lys-21 and Lys-262, and interactions involving Cys-298 stabilize the closed conformation of the enzyme·nucleotide complex (*9*, *35*). These key interactions are absent in CtXR: Asp-216 and Cys-298 of hAR are not positionally conserved in CtXR, and the putative nucleotide-enfolding loop of CtXR has a 4-amino-acid-long insertion at a position corresponding to Pro-215 and Asp-216 in hAR (*8*).

Reductase Property of CtXR and Other AKRs. The rate constant of hydride transfer from NADH to the carbonyl group of D-xylose (k_7) catalyzed by CtXR is much faster than the rate constant of the corresponding enzymatic hydride transfer from xylitol to NAD^+ (k_8). Hence, our kinetic characterization is used to classify CtXR as "reductase". The rate constant ratio, k_7/k_8, provides an estimate of 45 for the value of the bound-state equilibrium constant (K_{int}) at pH 7 and 25 °C. A even higher value of 217 was determined for K_{int} of NADPH-dependent reduction of D-xylose catalyzed by hAR (*9*). The actual rate constants of enzymic hydride transfer from NAD(P)H are much the same for yeast and human enzyme. These results strongly support the contention of a closely similar functional involvement of conserved catalytic-tetrad residues during aldehyde reduction catalyzed by CtXR and hAR. K_{int} of CtXR is considerably smaller than the external equilibrium constant (K_{ext}) of 520 for the NADH-dependent reaction in solution at pH 7. Therefore, this implies that, unlike hAR, CtXR has evolved enzymic mechanisms (such as differential binding of NADH vs NAD^+) to bring about a significant change of K_{int} relative to the value of the external reaction equilibrium constant (see later).

The results for CtXR are revealing with regard to catalysis by aldo-keto reductases in general. They show clearly that quasi-unidirectional hydride transfer to the carbonyl group of an aldehyde can be achieved with much the same efficiency from the very tight hAR·NADPH complex as well as from the 3200 (=16/0.005)-fold weaker, thus, probably less reactive CtXR·NADH complex. In case of the latter complex it would seem, however, that specific binding interactions with the natural sugar substrate are used to compensate for the smaller intrinsic reactivity toward aldehyde reduction. It is also interesting to compare the NAD(P)H-dependent reaction of CtXR and hAR with D-xylose, and the NADPH-dependent reaction of 3α-HSD with androstendione (*7*, *33*). While alcohol oxidation by CtXR and hAR occurs at slow rate relative to aldehyde reduction, turnover numbers of carbonyl reduction and alcohol oxidation by 3α-HSD are similar. Stopped-flow nucleotide binding studies conducted with 3α-HSD have provided evidence that nucleotide dissociation rates are not rate limiting in forward and reverse reaction of this enzyme (*33*), suggesting that chemistry may constitute the major rate-limiting step in either direction. Now, since X-ray structures have shown the closely similar configuration of catalytic tetrad residues of hAR (*11*) and 3α-HSD (*34*, *36*), the active-site machinery of aldo-keto reductases per se is not predisposed to determine unique catalytic properties of a "reductase". Subtle variations in enzyme structure, possibly proximal to the conserved tetrad,

may contribute to finely tune enzyme activities for functionning in oxidative or reductive direction.

Multiple Isotope Effects and Reaction Chemistry. The absence of a deuterium solvent isotope effect on k_{cat}/K_{xylose} and k_{cat} suggests that proton transfer which must occur during the reduction of an aldehyde to the corresponding primary alcohol is probably not a slow step of the NADH-dependent reduction of D-xylose catalyzed by CtXR. This finding is in good agreement with recent theoretical studies of D-glyceraldehyde reduction by hAR (*37*, *38*) in which the reduction process was shown to be determined primarily by hydride transfer while the energy barrier for the proton transfer was found to be very small (*37*, *38*).[5] The multiple deuterium isotope effect method was used to distinguish between concerted and stepwise mechanisms of hydride transfer and proton transfer in the CtXR-catalyzed reduction of D-xylose (*39*). If the reaction was concerted, hydride transfer and proton transfer would be independent of one another and thus equivalence of substrate isotope effects in H_2O and D_2O expected (*39*). When enzymatic reactions were carried out in D_2O, values of $^{D}(k_{cat}/K_{xylose})$ and $^{D}k_{cat}$ were smaller than corresponding isotope effects for reactions done in H_2O. Likewise, when using NADD in place of NADH, $^{D_2O}(k_{cat}/K_{xylose})_D$ and $^{D_2O}k_{catD}$ were inverse, indicating that substrate isotope effects and solvent isotope effects are not independent of one another. Therefore, deuteration of coenzyme to selectively slow the hydride transfer step and running the reaction in D_2O affect different steps in the mechanism of CtXR-catalyzed reduction of D-xylose; in other words, hydride transfer and proton transfer take place in a stepwise manner. In principle, the results do not allow to deduce which step comes first in the reaction mechanism of CtXR. However, it is chemically reasonable (see refs *4*, *37*, and *38*) to assume that (partial) formation of alcoholate by nucleophilic attack of hydride ion from NADH to the carbonyl group of the aldehyde precedes protonation of the oxygen atom of the alcoholate. In this scenario, the origin of the inverse solvent isotope effect on k_{cat}/K_{xylose} observed when using NADD is uncertain. However, a possible interpretation would be as follows. The phenolic side chain of Tyr has a fractionation factor or exchange equilibrium constant in D_2O (Φ) of 1.13 (*40*). By contrast, Φ values of most hydrogen bonds are ~1 (*40*). Now, although we would like to propose a rate-limiting transition state of aldehyde reduction by CtXR that is early with respect to proton transfer, hydrogen bonding interactions between the proton donor, likely Tyr-51, and the carbonyl oxygen of the aldehyde are expected to develop in the transition state of hydride transfer and cause polarization of the carbonyl group. The predicted solvent isotope effect for such a transition state would then be $\Phi_{reactant\ state}/\Phi_{transition\ state} = 1.13/1.0 = 1.13$, in however, only moderate agreement with our experimental observations (0.89).

Reduction of the Reactive Aldehyde Group of D-Glucosone. When in the presence of a system for enzymatic regeneration of NADH (*23*) the CtXR-catalyzed reduction of D-glucosone was allowed to proceed until substrate depletion was greater than 50%, a single product was detected which coeluted and comigrated with authentic D-fructose in HPLC and TLC, respectively (results not shown). Therefore, reported kinetic parameters and isotope effects pertain exclusively to the reduction of the aldehyde group in the dicarbonyl substrate. The α-carbonyl group of D-glucosone is expected to bring about a large increase in intrinsic chemical reactivity of the aldehyde toward reduction, relative to an aldehyde containing an α-hydroxy group. It has been shown by Penning and coworkers that nonenzymatic rates of NADPH-dependent reduction of dicarbonyls are $\sim 10^6$ times faster than corresponding rates of reduction of single-carbonyl compounds (*41*). For the enzymatic reaction catalyzed by CtXR, $^{D}(k_{cat}/K_{glucosone})$ was significantly smaller than $^{D}(k_{cat}/K_{xylose})$, indicating that the contribution of hydride transfer to rate limitation of the catalytic sequence is smaller for the reduction of D-glucosone, compared to reduction of D-xylose. However, differences in chemical reactivity between D-glucosone and D-xylose are not nearly expressed in the enzymatic rates and corresponding isotope effects on k_{cat}/K. Therefore, the presumably large propinquity effect of the α-carbonyl group appears to be efficiently eliminated at the active site of CtXR. Part of this differential rate enhancement in the enzymatic reactions with α-hydroxy and α-oxo aldehydes may be derived through positioning (for the general case, see ref *42*) in which the C-2 (*R*) hydroxy group of the substrate is thought to play a key role (*20*).

The observation of a solvent isotope effect on k_{cat} but not one on $k_{cat}/K_{glucosone}$ was unexpected. If the value for $^{D_2O}k_{cat}$ reflects partly rate-limiting proton transfer,[5] the absence of a solvent isotope effect on $k_{cat}/K_{glucosone}$ suggests a reaction of CtXR with D-glucosone in which proton and hydride transfer take place in two distinct steps whereby addition of the proton occurs after the first irreversible step of the reaction, likely hydride transfer.

Physiological Implications of Kinetic Data. The kinetic mechanism of CtXR is useful to analyze the role of the enzyme in D-xylose metabolism.

(1) The net rate constant of NAD^+ release by CtXR (18.6 s^{-1}) is approximately 100-fold faster thant the net rate of $NADP^+$ release by hAR (0.2 s^{-1}). This mostly explains the observed differences between yeast and human enzyme with respect to k_{cat} of D-xylose reduction and the fact that substrate specificity ($k_{cat}/K_{aldehyde}$) is partially expressed in the value of k_{cat} for the yeast enzyme.

(2) The relatively small variation in k_{cat}/K_{xylose} for CtXR and hAR while k_{cat} changes by 2 orders of magnitude as result of an evolutionary mechanism appears to be a manifestation of optimized enzyme-transition state complementarity in two aldo-keto reductases. The observed value of 100−200 $M^{-1}\ s^{-1}$ for k_{cat}/K_{xylose} mainly reflects constraints placed by the Haldane relationship for NAD(P)H-dependent aldehyde reduction catalyzed by two virtually unidirectional enzymes (see later). The observed 80-fold increase in K_{xylose} for CtXR, relative to hAR, mirrors the widely held principle

[5] It must be emphasized that a value of 4.73 was measured for $^{D_2O}(k_{cat}/K_{glyceraldehyde})$ in the reaction catalyzed by hAR (*5*). Results of theoretical studies by Kador and co-workers (*37*) are difficult to reconcile with these experimental findings. Varnai and Warshel (*38*) suggested that because the calculated energies of the transition states for hydride transfer and proton transfer in the stepwise reduction of D-glyceraldehyde by hAR lie close enough to each other (~2 kcal/mol), both steps may contribute to rate limitation of the catalytic cascade. However, in general one must be aware of the fact that the information contained in the observed solvent isotope effects may be complex and not necessarily disclose the presence or absence of rate limitation by the proton-transfer step.

of maximization of K_m in the evolution of enzymes of primary catabolism toward optimizing their reaction rates (*43*).

(3) Differential binding of NADH and NAD^+ in the steady state, reflected by a measured $K_{i,NADH}/K_{i,NAD^+}$ ratio of 0.082, is determined almost entirely by 10-fold difference in nucleotide "on" rates, thus $k_{14}/k_1 \approx 0.10$. By contrast, nucleotide "off" rate constants k_2 and k_{13}, and the rate constants for the conformational changes upon formation of the productive *E·NADH and *E·NAD^+ complexes contribute essentially nothing to the observed differential binding. The ratio of nucleotide binding constants (K_i) of CtXR mirrors closely the value of 0.15 for the prevailing intracellular ratio of [NADH]/[NAD^+] in yeast.[6] Thus, product inhibition of CtXR by NAD^+ will be small under physiological reaction conditions. When we assume a value of 110 μM for the intracellular concentration of NADH (*44*), the net rate constant of NADH binding, calculated according to k_1k_3 [NADH]/($k_2 + k_3$),[7] would be 55 s^{-1}. It is approximately 3 times the net rate constant of NAD^+ release. Comparison of second-order rate constants of NAD(P)H binding shows that formation of initial E·NADH complex occurs at rates 5−100-times slower than corresponding nucleotide on rates observed with other aldo-keto reductases (*9*, *10*, *33*).

(4) The intracellular ratio of [NADPH]/[NADH] that prevails in yeast during anaerobic growth on D-glucose, is approximately 2.8. Under these conditions, CtXR is expected to display a 18-fold preference of utilizing NADPH instead of NADH.[8] When D-xylose is the carbon source, the [NADPH]/[NADH] ratio is not known. However, because of excess NADH generated in the sugar assimilation process and NADPH consumed during reduction of D-xylose, this ratio is expected to have a value much smaller than 2.8. Then, the available NADPH will no longer outcompete the utilization of NADH.

(5) Although the concentration of free D-xylose in the yeast cytosol is not known, it is reasonable to assume that the rate of chemical transformation of D-xylose catalyzed by CtXR will be limited by the rate at which substrate combines productively with *E·NADH rather than by the rate of hydride transfer. The bimolecular rate constant of substrate binding (k_5) is, after correction for 0.02% free aldehyde present in aqueous solution of D-xylose (*45*), approximately 1.0×10^6 M^{-1} s^{-1}. This value is far below the rate expected of a diffusion-controlled process (10^8-10^9 M^{-1} s^{-1}). Therefore, this implies that k_5 may consist of a two-step sequence in which the actual binding of D-xylose is followed by a conformational change of the enzyme to bring about an optimal alignment of catalytic groups and reactants so as to allow subsequent hydride transfer to the carbonyl group. k_5 would thus be implicated in determining the substrate specificity of the enzyme. The fast net rate constant of hydride transfer ($k'_7 \approx k_7 = 170$ s^{-1}) ensures transformation into product of virtually all substrate molecules that have been bound productively.

(6) The bound-state equilibrium constant of CtXR strongly favors NADH-dependent reduction of D-xylose. This finding lends strong experimental support to the intuitive suggestion of a metabolically unidirectional function of XR in physiology of *C. tenuis*.

ACKNOWLEDGMENT

Prof. C. Obinger (Institute of Chemistry, BOKU) kindly provided access to the stopped-flow intrument in his laboratory. The invaluable support and expert assistance of Drs. P.-G. Furtmüller and U. Burner in acquiring transient kinetic data is gratefully acknowledged.

REFERENCES

1. Bohren, K. M., Bullock, B., Wermuth, B., and Gabbay, K. H. (1989) *J. Biol. Chem. 264*, 9547−9551.
2. Jez, J. M., Bennett, M. J., Schlegel, B. P., Lewis, M., and Penning, T. M. (1997) *Biochem. J. 326*, 625−636.
3. Jez, J. M., Flynn, T. G., and Penning, T. M. (1997) *Biochem. Pharmacol. 54*, 631−639.
4. Penning, T. M. (1999) *J. Steroid Biochem. Mol. Biol. 69*, 211−235.
5. Bohren, K. M., Grimshaw, C. E., Lai, C.-J., Harrison, D. H., Ringe, D., Petsko, G. A., and Gabbay, K. H. (1994) *Biochemistry 33*, 2021−2032.
6. Tarle, I., Bohrani, D. W., Wilson, D. K., Quiocho, F. A., and Petrash, M. (1993) *J. Biol. Chem. 268*, 25687−25693.
7. Schlegel, B. P., Jez, J. M., and Penning, T. M. (1998) *Biochemistry 37*, 3538−3548.
8. Nidetzky, B., Mayr, P., Neuhauser, W., and Puchberger, M. (2000) *Chem. Biol. Interact. 130−132*, 583−595.
9. Grimshaw, C. E., Bohren, K. M., Lai, C.-J., and Gabbay, K. H. (1995) *Biochemistry 34*, 14356−14365.
10. Kubiseski, T. J., Hyndman, D. J., Morjana, N. A., and Flynn, G. T. (1992) *J. Biol. Chem. 267*, 6510−6517.
11. Wilson, D. K., Bohren, K. M., Gabbay, K., and Quiocho, F. A. (1992) *Science 257*, 81−84.
12. Bohrani, D. W., Harter, T. M., and Petrash, J. M. (1992) *J. Biol. Chem. 267*, 24841−24847.
13. Rondeau, J.-M., Tete-Favier, F., Podjarny, A., Reymann, J.-M., Barth, P., Biellmann, J.-F., and Moras, D. (1992) *Nature 355*, 469−472.
14. Wilson, D. K., Tarle, I., Petrash, J. M., and Quiocho, F. A. (1993) *Proc. Natl. Acad. Sci. U.S.A. 90*, 9847−9851.
15. Urzhumtsev, A., Tete-Favier, F., Mitschler, A., Barbanton, J., Barath, P., Urzhumtsev, L., Biellman, J.-F., Podjamy, A. D., and Moras D. (1997) *Structure 5*, 601−612.
16. Harrison, D. H., Bohren, K. M., Ringe, D., Petsko G. A., and Gabbay, K. H. (1994) *Biochemistry 33*, 2011−2020.
17. Harrison, D. H., Bohren, K. M., Petsko, G. A., Ringe, D., and Gabbay, K. H. (1997) *Biochemistry 36*, 16134−16140.
18. Grimshaw, C. E. (1992) *Biochemistry 31*, 10139−10145.
19. Neuhauser, W., Haltrich, D., Kulbe, K. D., and Nidetzky, B. (1997) *Biochem. J. 326*, 683−692.
20. Neuhauser, W., Haltrich, D., Kulbe, K. D., and Nidetzky, B. (1998) *Biochemistry 37*, 1116−1123.
21. Nidetzky, B., Mayr, P., Hadwiger, P., and Stütz, A. E. (1999) *Biochem. J. 344*, 101−108.
22. Mostad, S. B., and Glasfeld, A. (1993) *J. Chem. Ed. 70*, 504−506.
23. Leitner, C., Neuhauser, W., Volc, J., Kulbe, K. D., Nidetzky, B., and Haltrich, D. (1998) *Biocat. Biotrans. 16*, 365−382.
24. Schowen, K. B., and Schowen, R. L. (1982) *Methods Enzymol. 87*, 551−606.
25. Frieden, C. (1994) *Methods Enzymol. 240*, 311−322.
26. Northrop, D. B. (1982) *Methods Enzymol. 87*, 607−625
27. Cleland, W. W. (1990) in *The Enzymes* (Boyer, P. D., and Krebs, E. G., Eds.) pp 99−158, 3rd. ed., Academic Press, San Diego.
28. Cook, P. F., Blanchard, J. S., and Cleland, W. W. (1980) *Biochemistry 19*, 4853−4858.

[6] Data are for baker's yeast grown anaerobically and using D-glucose as carbon source (*44*). We assume a value of 0.25 for the ratio of dry to wet yeast biomass.

[7] The expression is for saturating [D-xylose]. If [D-xylose] is not saturating, k_3 is replaced by k'_3 which depends on [D-xylose].

[8] The value was calculated according to (k_{cat}/K_{NADPH}) 2.8/(k_{cat}/K_{NADH}), employing kinetic parameters from Neuhauser et al. (*19*).

29. Pettersson, G. (1976) *Eur. J. Biochem. 69*, 273−278.
30. Sekhar, V. C., and Plapp, B. V. (1988) *Biochemistry 27*, 5082−5088.
31. Kvassman, J., and Pettersson, G. (1976) *Eur. J. Biochem. 69*, 279−287.
32. Cook, P. F. (1991) in *Enzyme Mechanism From Isotope Effects* (Cook, P. F., Ed.) pp 203−245, CRC Press, Boca Raton.
33. Ratnam, K., Ma, H., and Penning, T. M. (1999) *Biochemistry 38*, 7856−7864.
34. Benett, M. J., Schlegel, B. P., Jez, J. M., Penning, T. M., and Lewis, M. (1996) *Biochemistry 35*, 10702−10711.
35. Grimshaw, C. E., Bohren, K. M., Lai, C.-J., and Gabbay, K. H. (1995) *Biochemistry 34*, 14374−14384.
36. Benett, M. J., Albert, J. M., Jez, J. M., Ma, T. M., Penning, T. M., and Lewis, M. (1997) *Structure 5*, 799−812.
37. Lee, Y. S., Hodoscek, M., Brooks, B. R., and Kador, P. F. (1998) *Biophys. Chem. 70*, 203−216.
38. Varnai, P., and Warshel, A. (2000) *J. Am. Chem. Soc. 122*, 3849−3860.
39. Cleland, W. W. (1991) in *Enzyme Mechanism From Isotope Effects* (Cook, P. F., Ed.) pp 247−265, CRC Press, Boca Raton.
40. Quinn, D. M., and Sutton, L. D. (1991) in *Enzyme Mechanism From Isotope Effects* (Cook, P. F., Ed.) pp 73−126, CRC Press, Boca Raton.
41. Schlegel, B. P., Ratnam, K., and Penning, T. M. (1998) *Biochemistry 37*, 11003- 11011.
42. Jencks, W. P. (1975) *Adv. Enzymol. 43*, 219−410.
43. Fersht, A. (1999) *Structure and mechanism in protein science*, Freeman, San Fransisco.
44. Anderlund, M., Nissen, T. L., Nielsen, J., Villadsen, J., Rydström, J., Hahn- Hägerdal, B., and Kielland-Brandt, M. C. (1999) *Appl. Environm. Microbiol. 65*, 2333−2340.
45. Hayward, L. D., and Angyal, S. J. (1977) *Carbohydr. Res. 53*, 13−20.
46. Cleland, W. W. (1975) *Biochemistry 14*, 3220−3224.

BI010148A